

1 **Biogas to LBG via Cryogenic Upgrading Technologies**

2
3 Laura Annamaria Pellegrini^a, Giorgia De Guido^{a,*}, Stefano Langé^a

4
5 Email addresses: laura.pellegrini@polimi.it, giorgia.deguido@polimi.it, stefano.lange@polimi.it

6
7 ^a *Dipartimento di Chimica, Materiali e Ingegneria Chimica “Giulio Natta”, Politecnico di Milano -*
8 *Piazza Leonardo da Vinci, I-20133, Italy*

9
10 *Corresponding author: Giorgia De Guido

11 Tel.: +39 02 2399 3260

12 E-mail address: giorgia.deguido@polimi.it

13 Full postal address: Dipartimento di Chimica, Materiali e Ingegneria Chimica “G. Natta”, Politecnico di
14 Milano, Piazza Leonardo da Vinci 32, I-20133, Milano, Italy

15 16 **Abstract**

17 Liquid biomethane (LBM), also referred to as liquid biogas (LBG), is a promising biofuel for
18 transport that can be obtained from upgrading and liquefaction of biogas. With respect to fossil
19 fuels, LBM is a renewable resource, it can be produced almost everywhere, and it is a carbon
20 neutral fuel. With respect to compressed biomethane (CBM), LBM is a 3 times more energy dense
21 fuel and it allows longer vehicle autonomy. With respect to other transport biofuels, LBM has also a
22 higher energy density, it is produced from wastes and recycled material without being in
23 competition with food production, and it assures a high final energy/primary energy ratio. The low
24 temperatures at which LBM is obtained strongly suggest the use of cryogenic technologies also for
25 biogas upgrading. In addition, it is well proved in the literature on natural gas purification (indeed
26 biogas can be considered as a “particular” natural gas with a high CO₂ content) that cryogenic
27 technologies and, in particular, cryogenic distillation are less energy consuming when compared to
28 traditional technologies such as amine washing for CO₂ removal. Low-temperature purification
29 processes allow the direct production of a biomethane stream at high purity and at low temperature,
30 suitable conditions for the direct synergistic integration with biogas cryogenic liquefaction

31 processes, while CO₂ is obtained in liquid phase and under pressure. In this way, it can be easily
32 pumped for transportation, avoiding significant compression costs as for classical CO₂ capture units
33 (where carbon dioxide is discharged in gas phase and at atmospheric pressure).

34 In this paper, the three most common natural gas low-temperature purification technologies have
35 been modelled and their performances have been evaluated through energy consumption analysis
36 and comparison, in terms of the equivalent amount of methane required for the upgrading, with the
37 amine washing process, proving the profitability of cryogenic technologies. Specifically, the Ryan-
38 Holmes, the dual pressure low-temperature distillation process and the anti-sublimation process
39 have been considered. It has been found that the dual pressure low-temperature distillation scheme
40 reaches the highest thermodynamic performances, resulting in the lowest equivalent methane
41 requirement with respect to the other configurations. This is mainly due to the distributed
42 temperature profile along a distillation column that differs from a reversible heat exchange process
43 to a lesser extent.

44

45 **Keywords:** *biogas upgrading, LBG, low-temperature, distillation, MEA, energy saving*

46

47 **1. Introduction**

48 Biomethane is methane sourced from renewable biomass. The pre-stage of biomethane is better
49 known as biogas, which is produced by anaerobic digestion of organic material, such as manure,
50 sewage sludge, the organic fractions of household and industry waste, and energy crops [1]. Biogas
51 is also produced during anaerobic fermentation in landfills and is then referred to as landfill gas.

52 The worldwide biogas production is unknown, but the production of biogas in the European Union
53 in 2013 accounted for 13.4 million tons of oil equivalent (10% increase compared to 2012), which
54 represented 52.3 TWh of electricity produced and net heat sales to heating district networks of 432
55 megatons of oil equivalent [2].

56 The composition of biogas depends on the organic matter present in the waste and on the type of
57 anaerobic digestion process, which in turn depends on the origin of the residue digested [3]. For
58 instance, biogas obtained from the anaerobic degradation of sewage sludge, livestock manure or
59 agroindustrial biowastes contains 53-70% of CH₄ and 30-47% of CO₂ [4-6] together with other
60 impurities.

61 Biogas can be utilized as a fuel for on-site heat, steam and electricity generation in industry, as a
62 substrate in fuel cells, as a substitute of natural gas for domestic and industrial use prior to injection

63 into natural gas grids and as a vehicle fuel [7-9]. Depending on the end use, different biogas
64 treatment steps are necessary. When it is important to have a high energy gas product, *e.g.* as
65 vehicle fuel or for grid injection, the gas needs to be upgraded, *i.e.* CO₂ must be removed.

66 Upgrading of biogas has gained increased attention due to increasing targets for renewable fuel
67 quotes for vehicles in many countries. As a matter of fact, biofuels serve as a renewable alternative
68 to fossil fuels in the EU's transport sector, helping to reduce greenhouse gas emissions and to
69 improve the EU's security of supply. By 2020, the EU aims to have 10% of the transport fuel of
70 every EU country come from renewable sources such as biofuels.

71 When the end use of biomethane is as a vehicle fuel, the conversion into liquid biogas (LBG) can be
72 profitable: indeed, LBG is more than 600 times space efficient compared to biogas at atmospheric
73 pressure and around 3 times more space efficient compared to compressed biogas (CBG) at 200 bar.
74 There are two main ways to produce LBG, namely cryogenic/low-temperature upgrading
75 technologies, where the purified gas is obtained directly at low temperatures, and conventional
76 upgrading technologies (water scrubbing, chemical scrubbing, PSA, membranes) [10-12] coupled to
77 a small-scale liquefaction plant. Since biogas can be considered as a particular natural gas with a
78 high CO₂ content, the results already available in the literature on natural gas purification can be
79 taken into account, which suggest that low-temperature processes, and in particular those based on
80 distillation, require less energy than conventional purification technologies, such as amine
81 scrubbing [13].

82 This work compares the performances of three biogas upgrading technologies operated at low
83 temperatures, namely the Ryan-Holmes extractive distillation process [14, 15], a recently developed
84 dual pressure low-temperature distillation process [16] and the anti-sublimation process [17], with
85 those of a conventional purification process, based on the use of a monoethanolamine (MEA)
86 aqueous solution. It will be shown that the use of cryogenic/low-temperature technologies is
87 synergistic with the cryogenic temperature (about -160°C) required for LBG production, resulting
88 in energy savings for the overall process. Another advantage in using cryogenic/low-temperature
89 technologies is that CO₂ is obtained as a clean liquid product that could be used in external
90 applications.

91

92 **2. Description of process solutions**

93 For all the considered process solutions, feed and products conditions are the same in order to better
94 perform the comparison on an energy basis. The feed stream is raw biogas at 35°C and 1 atm. The
95 composition is 40 mol% of CO₂ and 60 mol% of CH₄. The final biomethane has been considered as
96 liquid at atmospheric pressure, with a CO₂ content below 50 ppm, as recommended for LNG

97 production [18] to avoid freezing problems during liquefaction. For the produced CO₂ stream, the
98 mole fraction of CH₄ has been set to 1.0e-4 in order to enhance the methane recovery and to
99 maintain the same standards adopted for the design of the dual pressure low-temperature distillation
100 process [16]. Regarding its final conditions, the goal is to obtain it in liquid phase under pressure
101 (50 bar), which makes it suitable for further uses. No dehydration steps have been considered in any
102 case, neither for low-temperature technologies nor for the MEA scrubbing process, since all of them
103 require to remove water either before or after the upgrading step. Indeed, for the MEA scrubbing
104 process water is removed after the purification section since it is given by saturation conditions at
105 the outlet of the absorber. On the contrary, for the low-temperature distillation processes water is
106 removed before the upgrading step: in this case, the water content of the raw biogas is not known *a-*
107 *priori* since it is related to previous treatments. Generally, biogas compression will help to remove
108 part of the water by condensation and, thus, a subsequent step to remove water will be needed to
109 reach the final specifications for low-temperature processing. Also in the anti-sublimation process
110 water has to be captured to avoid that water vapor freezes on the low temperature evaporators,
111 blocking the flue gases passages: this is accomplished at successive levels of temperature, first by
112 condensation and then by a frosting/defrosting process.

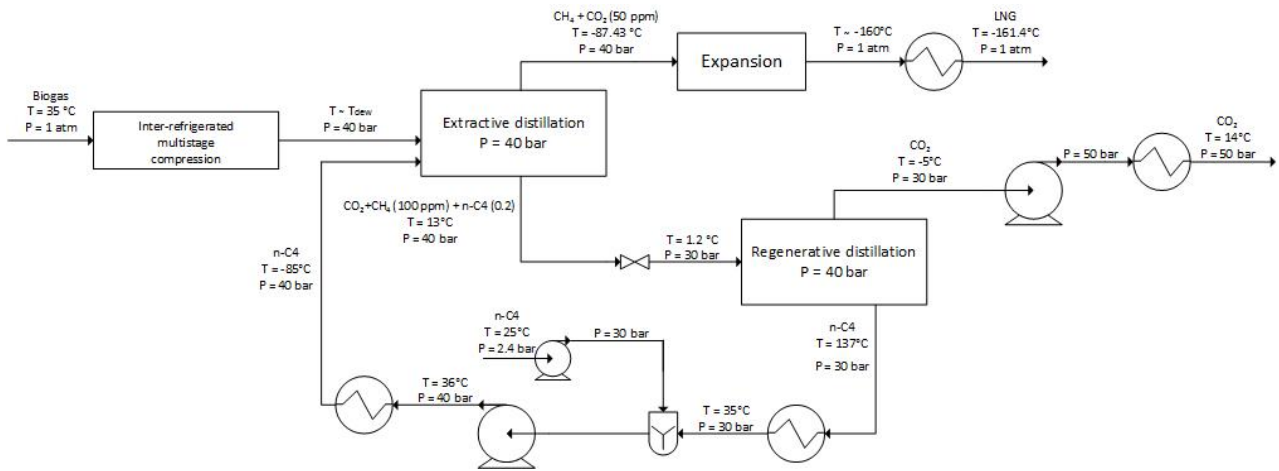
113 The complete process simulation has been performed only for the low-temperature processes, while
114 for the amine sweetening unit widely used and tested rules of thumb have been employed to
115 estimate the major energy costs related to the purification part, so for the scheme with upgrading by
116 MEA scrubbing only the biomethane and CO₂ liquefaction trains have been simulated. Process
117 simulations have been performed with the commercial process simulator Aspen Hysys® [19], using
118 the SRK equation of state [20], which is suitable to represent the phase behavior of these kinds of
119 mixtures commonly found in the gas industry. The number of theoretical stages used for the
120 distillation columns in each process scheme has been chosen in order to take into account a
121 qualitative trade-off between energy consumptions and capital costs. The selection of the number of
122 theoretical trays starts from literature case studies [16, 21].

123

124 **2.1 The Ryan-Holmes process**

125 The Ryan-Holmes process [14, 15] performs the removal of carbon dioxide by means of an
126 extractive distillation in order to increase the critical locus of the CH₄-CO₂ system and, at the same
127 time, to move the freezing line to lower temperatures and pressures. Normally, hydrocarbons
128 heavier than methane are used as entrainer and, in particular, n-butane [14, 15, 21]. The process
129 scheme is illustrated in Fig. 1.

130



131

132 **Fig. 1.** Process Flow Diagram of the Ryan-Holmes process.

133

134 The unit consists of five main parts: the biogas compression section (*Inter-refrigerated multistage*
 135 *compression*), the extractive distillation unit (*Extractive distillation*), the entrainer regeneration
 136 section (*Regenerative distillation*), the biomethane liquefaction train (*Expansion*, followed by the
 137 final heat exchanger) and the CO₂ pump. The process should be operated under pressure for
 138 different reasons: to remain above the CO₂ triple point pressure in order to guarantee the presence
 139 of a liquid phase rich in carbon dioxide; to increase the operating temperatures, so reducing the
 140 refrigeration costs, and to keep the pressure sufficiently high in order to favor the solubility of CO₂
 141 in the liquid phase (remaining above the freezing point of CO₂ in mixture with methane and n-
 142 butane). For this reason, the inlet biogas feed at 35°C is compressed from atmospheric pressure to
 143 about 40 bar before entering the extractive distillation section. The demethanizer column
 144 (*Extractive distillation*) is co-fed with n-butane as additive to avoid CO₂ freezing and to increase the
 145 distillation performances. This first distillation column has 40 theoretical trays. The position of the
 146 feed, at the 18th stage from the top, has been chosen in order to minimize the required duties, while
 147 the entrainer is fed on the third tray from the top of the distillation column to avoid its entrainment
 148 in the produced stream. The n-butane flow rate is 10 moles/100 moles of feed [21]. The entrainer
 149 stream (*n-C4*) conditions have been fixed in order to create the minimum discontinuity in column
 150 profiles: its temperature and pressure levels (-85°C, 40 bar) have been chosen to be close to the
 151 ones obtained on the third tray of the distillation column (*Extractive distillation*). The *Extractive*
 152 *distillation* top product stream is then sent to the liquefaction train, to obtain the final liquefied
 153 biomethane product stream (*LNG*). The bottom product stream from the *Extractive distillation*
 154 section contains CO₂ and the entrainer. This stream is expanded to 30 bar, to remain under the n-
 155 butane critical pressure, and needs a further treatment to recover separately CO₂ and n-butane, the
 156 latter to be recycled to the *Extractive distillation* unit. The *Regenerative distillation* unit has been

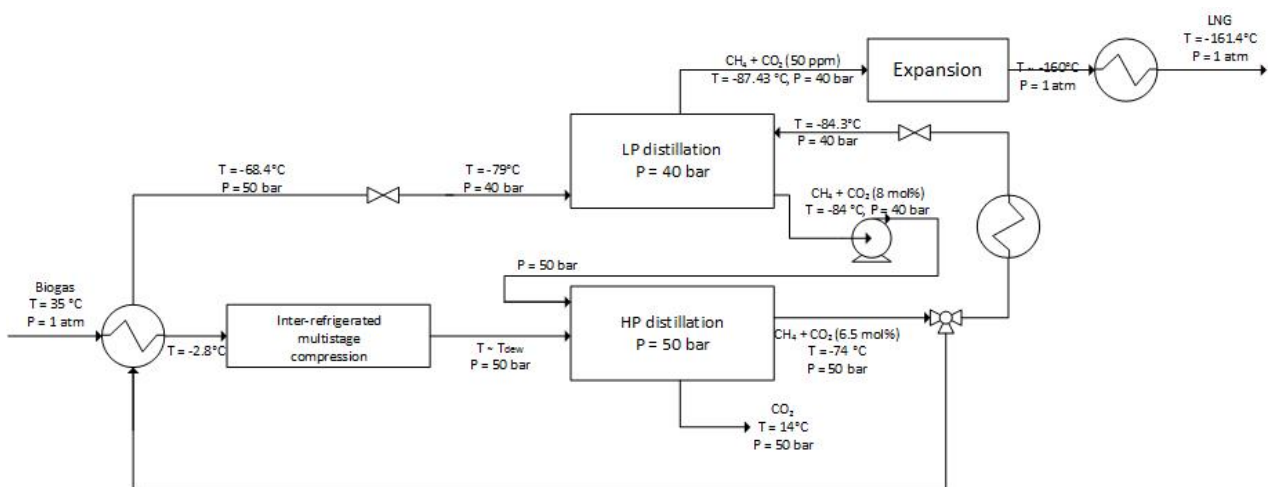
157 used to separate carbon dioxide from n-butane, using 40 theoretical trays. The compressed biogas
 158 stream is suitable to be fed on the 31st stage from the top. On the top of the regeneration column, the
 159 distillate is rich in CO₂ and is obtained in liquid phase by means of a total condenser. To reach the
 160 desired conditions for the CO₂ final stream, the liquid product stream from the top of the
 161 *Regenerative distillation* section needs to be pumped to 50 bar before being heated up to 14.06°C.
 162 The bottom stream from this column contains mainly n-butane, which has to be recycled to the
 163 *Extractive distillation* section. To ensure the conditions required by the process, this stream has to
 164 be integrated with an appropriate make-up stream, pumped and cooled down to the desired
 165 conditions. This process is considered to belong to the class of low-temperature separation
 166 processes because of the temperature profile established in the *Extractive distillation* unit: the
 167 temperature decreases from 13.06°C at the bottom reboiler down to -87.3°C at the top condenser.
 168 The regeneration column operates at higher temperature levels: the condenser temperature is close
 169 to -5.5°C and the bottom one is 137°C. Therefore, the energy demand for the extractive distillation
 170 is mainly determined by the condenser duty, while the reboiler duty plays the most significant role
 171 for the regeneration column. The final biomethane is liquefied through an isentropic expansion in a
 172 flashing liquid expander [22] followed by a final condenser, that allows to obtain biomethane in
 173 liquid phase and at atmospheric pressure.

174

175 2.2 The dual pressure low-temperature distillation process

176 In the scheme reported in Fig. 2, the upgrading of raw biogas is performed by means of a dual
 177 pressure low-temperature distillation process [16].

178



179

180 **Fig. 2.** Process Flow Diagram of the dual pressure low-temperature distillation process.

181

182 In this process, the purification section consists of two distillation units: the first one is operated at

183 high pressure (*HP distillation*, 50 bar), above the maximum of the freezing line of CO₂ in mixtures
184 with methane, while the second one at low pressure (*LP distillation*, 40 bar), below the methane
185 critical pressure. The number of theoretical trays for these two distillation units is 25 and 20,
186 respectively. The HP section can be conceived as the stripping section of a common distillation
187 column: it presents only a reboiler, while the liquid reflux is provided by recycling the liquid stream
188 coming from the bottom of the LP section. In the same way, the LP section works as the enrichment
189 section of a classic distillation column: it has a partial condenser at the top and the gas feed stream
190 is the top product of the HP section. The produced gas stream from the top of the LP section is
191 methane at the required purity specification. Liquid biomethane is then produced by means of a
192 proper liquefaction train. It has been assumed that this section consists of a gas turbine followed by
193 a cooler as considered for the Ryan-Holmes process. The bottom product from the *HP distillation*
194 section is highly pure carbon dioxide. The biogas feed stream is precooled in a first heat exchanger
195 that uses the available cooling duty of an intermediate process stream, which needs to be heated
196 before being fed to the LP section. The precooled biogas is then compressed to 50 bar and further
197 cooled down to its dew point at 50 bar, before entering the *HP distillation* section. The compression
198 is performed after the precooling of the biogas in order to reduce the compression power by
199 decreasing the temperature of the inlet feed stream. According to the phase behavior of the CO₂-
200 CH₄ mixture [23], no freezing can occur during distillation at about 50 bar. The HP section
201 performs a bulk removal of the inlet CO₂: the bottom stream is liquid CO₂ at high pressure, while
202 the top product stream is a methane-rich gas stream (with about 6.5 mol% of CO₂). Since the HP
203 section operates at a pressure above the methane critical one (45.9 bar), it is not possible to obtain
204 pure methane by performing the distillation in a single unit operated at 50 bar. The final purification
205 is performed in the LP section, operated at about 40 bar. The produced streams from the LP section
206 are a top methane gas stream and a bottom methane-rich liquid stream that is pumped back to the
207 HP section. The feed stream enters the HP section on the fourth tray from the top, while the liquid
208 reflux, coming from the bottom of the LP section, is pumped and fed on the first tray from the top.
209 The top gas stream from the HP section is sent to a splitter, which separates it into two streams.
210 Before entering the bottom of the LP section, a part of the HP section top product stream is heated
211 up and expanded to the LP section pressure, so that it is at a temperature 5-6 K higher than its dew
212 point temperature at the pressure of the LP section. This guarantees that no solid phase is formed
213 during the expansion. The heat needed for this operation is taken from the inlet raw biogas stream
214 that is precooled before the compression train. The remaining part of the HP section top product
215 stream is cooled down at 50 bar (away from the CO₂ solubility boundary) and expanded to the LP
216 section pressure in order to obtain a liquid stream at its bubble point, which is fed to the LP section

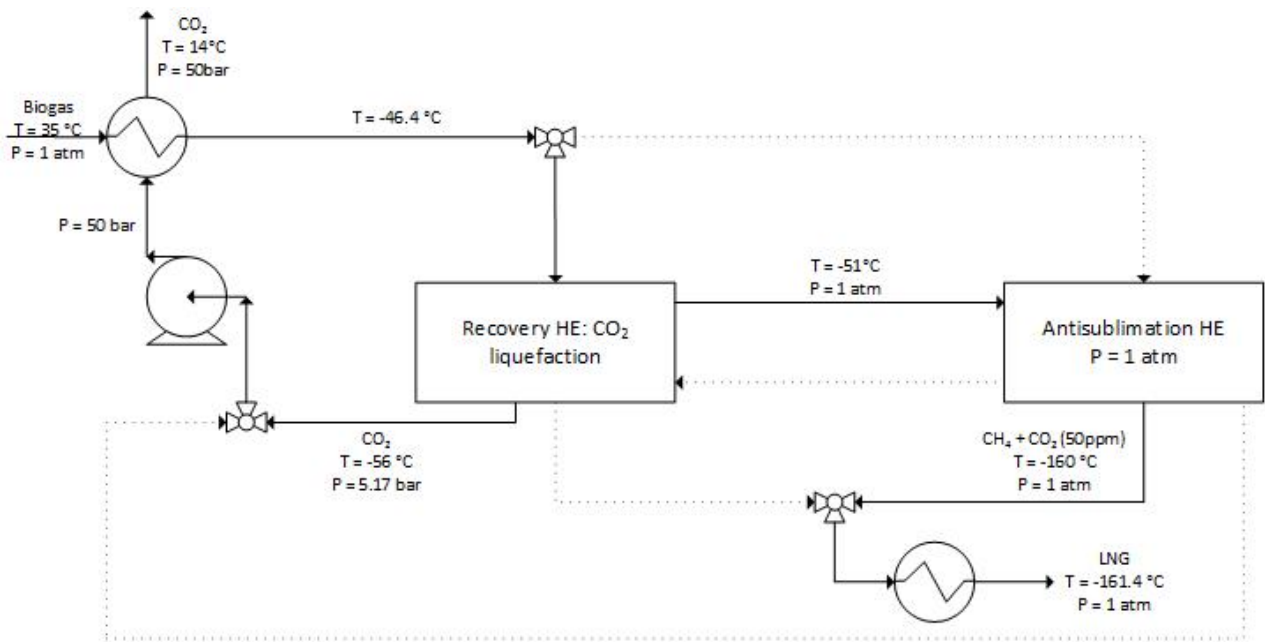
217 one theoretical tray above the gas feed stream. The split factor of the HP section top product stream
 218 is chosen in order to keep the CO₂ level below 8 mol% in the LP section bottom product stream for
 219 avoiding CO₂ freezing. The reflux ratio for the LP distillation has been set to about 2.4.

220

221 2.3 The anti-sublimation process

222 The liquefied biomethane production by means of the anti-sublimation process [17, 24] employs
 223 heat exchanger surfaces to upgrade the biogas operating in the solid-vapor equilibrium region [23]
 224 at atmospheric pressure: CO₂ is frosted from the gas stream that is, consequently, enriched in
 225 methane. The scheme adopted for this process is shown in Fig. 3.

226



227 **Fig. 3.** Process Flow Diagram of the anti-sublimation process.

228

229 In the anti-sublimation process the purification is performed allowing dry ice formation in a closed
 230 and dedicated unit operation. In the scheme illustrated in Fig. 3, two heat exchangers are operated in
 231 dynamic mode, carrying out the purification (Anti-sublimation Heat Exchanger, hereafter denoted
 232 by AHE) and the regeneration (Recovery Heat Exchanger, hereafter denoted by RHE) phases
 233 switching the flow path through these two equipment, ensuring the continuous operation of the
 234 process. Different line styles (solid and dotted) have been adopted in order to describe the material
 235 flows direction according to the working phase alternation: solid lines are used for the operation
 236 phase, while dotted lines denote the regeneration one. The raw biogas stream is fed to the process at
 237 35°C and atmospheric pressure. The stream is sent to a heat exchanger, where it is cooled down by
 238 means of cold recovery from the liquefied CO₂ coming from RHE. The amount of heat recovery is
 239 defined in order to warm the liquid CO₂ stream up to 14°C at 50 bar, assuming a minimum

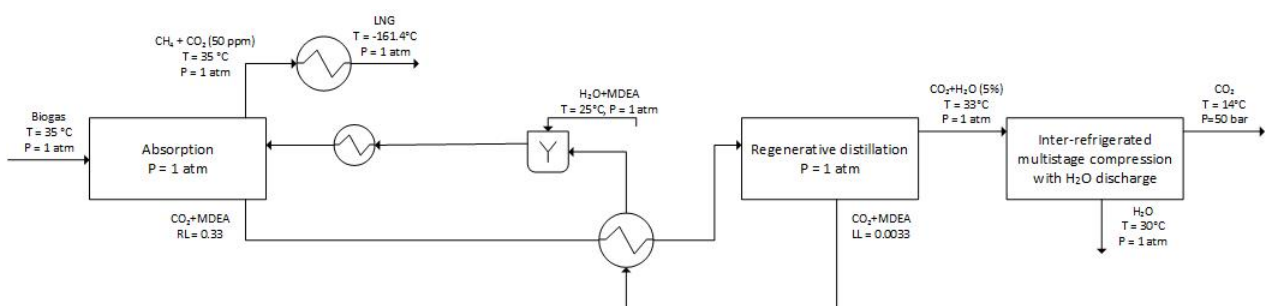
240 temperature approach of about 5 K. The cold biogas is fed to the RHE. The dry ice layer deposited
 241 during the previous operating cycle, when the RHE worked as AHE, provides part of the cooling
 242 duty to the biogas stream and this allows to reach temperatures down to -51°C by melting the dry
 243 ice that is recovered as liquid CO_2 at its triple point. In order to avoid pinch problems, a minimum
 244 approach equal to 5 K is kept between the temperatures of the outlet cold biogas and of the liquid
 245 CO_2 . The liquid CO_2 stream is then pumped to 50 bar and heated in a heat recovery equipment. The
 246 cold biogas from the RHE is then fed to the anti-sublimation heat exchanger (AHE). To achieve
 247 CO_2 anti-sublimation a supplementary cooling power is necessary to decrease the temperature ($-$
 248 160°C) and frost CO_2 to ensure the desired specification on the final product. The cooling duty
 249 necessary to perform this operation is supplied by an external refrigeration cycle. Inside the AHE, a
 250 solid CO_2 layer grows and a gas stream with 50 ppm of CO_2 is available at atmospheric pressure.
 251 The produced gas is then liquefied for the final purpose. A heat exchanger using an external cooling
 252 medium is used for this scope. Once the RHE is cleaned and ready to support dry ice formation and
 253 the AHE presents a solid CO_2 layer that needs to be liquefied and recovered, a switch between the
 254 RHE and the AHE is performed to assure the continuity of the purification and liquefaction
 255 operation. Since the formation of a CO_2 solid phase occurs, the anti-sublimation process has been
 256 simulated according to heat and material balances across the RHE and the AHE sections [23].

257

258 2.4 The chemical absorption process

259 The fourth considered process solution, illustrated in Fig. 4, is a conventional chemical scrubbing
 260 process with an aqueous MEA solution as solvent. For applications at low pressures, such as carbon
 261 capture from power plant flue gases, MEA is typically preferred to other amines as chemical
 262 solvent, since it shows faster CO_2 absorption kinetics also at low pressure [25].

263



264 **Fig. 4.** Process Flow Diagram of the MEA scrubbing process.

265

266 The biogas feed is sent to the absorption column (*Absorption*), where it is contacted
 267 countercurrently with the lean MEA solution. The purified gas stream is obtained at the top of the
 268 absorber and a rich liquid stream at the bottom, containing the CO_2 to be removed. The rich stream

269 is heated in the intermediate cross heat exchanger and sent to the regeneration column
 270 (*Regenerative distillation*), where CO₂ is stripped from the solvent and obtained as gas at the top,
 271 while the lean regenerated solvent is recovered at the bottom of the column. The hot lean stream is
 272 cooled in the intermediate cross heat exchanger and is further cooled before being recycled to the
 273 absorber. The intermediate heat exchanger is used to favour the internal process heat recovery.
 274 Make-up of water and amine is needed due to leakages occurring during solvent regeneration. To
 275 reduce the make-up, the regenerator condenser can be operated at the lowest possible temperature
 276 compatible with the available utilities (30°C has been assumed in this work, which is in the range
 277 typically reported in the literature [26], *i.e.* 30-50°C).
 278 In this work, a 30 wt% amine aqueous solution has been assumed as solvent.
 279 The rich loading (*RL*) has been selected to be 0.33 (moles of CO₂ per moles of MEA) [25, 27]. The
 280 limiting value of the rich loading is selected considering the lifetime of the plant. The rich solution
 281 is highly corrosive due to the presence of dissociated acidic electrolytes in the aqueous solutions
 282 and a reasonable value is generally fixed from the experience on existing purification units.
 283 The lean solvent is regenerated to obtain an acid lean loading (*LL*) equal to 1/100 of the rich loading
 284 [26].
 285 Heat to the reboiler of the regeneration column is supplied using low-pressure steam at 3.5 bar. In
 286 the literature, several useful correlations to estimate energy consumptions, particularly regarding
 287 process heat supplied to the reboiler of the regeneration column, are available [25, 27]. Compared
 288 to the other studied process solutions, this last scheme typically operates at ambient or higher
 289 temperatures. In this way, the higher costs are related to the solvent regeneration column.
 290 Generally, according to rules of thumb, linear relations between steam consumptions (and, thus,
 291 thermal power) and the volumetric flow rate of the circulating solvent (that takes into account the
 292 effect of the inlet CO₂ content of the raw gas) can be used for the estimation of the reboiler duty.
 293 The rule of thumb adopted in this work assumes that the proportionality constant, *K*, giving the
 294 consumption of LP steam per m³ of lean circulating solution is equal to 120 kg/m³ [25, 27].
 295 To determine the lean amine flow rate, it is necessary to calculate the amount of the absorbed acid
 296 gas (CO₂) to purify the raw biogas stream to the required specification. Knowing the raw biogas
 297 flow rate and composition, it is possible to compute the molar flow of the absorbed acidic
 298 compound from eq. (1), where $x_{CO_2}^{SPEC}$ is the specification for CO₂ in the purified gas at the absorber
 299 outlet.

$$mol_{CO_2}^{ABSORBED} = mol_{CO_2}^{IN} - \frac{mol_{CH_4}^{OUT} \left(x_{CO_2}^{SPEC} \right)}{1 - x_{CO_2}^{SPEC}} \quad (1)$$

300 The MEA aqueous solvent flow rate can be so determined knowing the total molar flow of the
 301 absorbed acid gas, the rich loading of 0.33 and the lean loading of 0.0033. In this way, the
 302 difference between the rich and the lean loadings is the ratio between the absorbed CO₂ and the
 303 moles of amine in the solvent. It is so possible to calculate the molar flow rate of MEA in the
 304 aqueous solution (eq. (2)) and, therefore, the molar flow rate of the solvent.

$$mol_{MEA} = \frac{mol_{CO_2}^{ABSORBED}}{RL - LL} \quad (2)$$

305 To calculate the steam consumption at the reboiler, it is necessary to determine the volumetric flow
 306 rate of the circulating lean solvent from eq. (3), where the molar concentration (C_{MEA}) of the solvent
 307 (44 kmol/m³ at 30°C and 1 atm) is calculated from the densities of MEA and water.

$$Volume_{Solvent} = \frac{mol_{Solvent}}{C_{MEA}} \quad (3)$$

308 It is then possible to determine both steam consumption and the duty at the regeneration column
 309 reboiler, through eq. (4) and eq. (5), respectively.

$$Steam = Volume_{Solvent} \cdot K \quad (4)$$

$$Duty = Steam \cdot \Delta H_{Ev, H_2O}^{3.5bara} \quad (5)$$

310 In eq. (5) $\Delta H_{Ev, H_2O}^{3.5bara}$ is the mass latent heat of vaporization of water at 3.5 bara and its value is 2148
 311 kJ/kg at a boiling temperature of 140°C [28].

312 The liquid biomethane production is performed by direct cooling since the gas is available at
 313 atmospheric pressure, assuming that the dehydration of the produced gas is not taken into account,
 314 as previously stated. Since from the top of the regeneration column the CO₂ is obtained wet and at
 315 low pressure, to reach the same conditions of the other schemes some additional treatments are
 316 necessary, which include a compression train, condensates separation and final cooling.

317 The intercooled compression has been designed considering three stages and the outlet pressure
 318 from each compression stage has been calculated according to eq. (6), where P_{out}/P_{in} is the global
 319 compression ratio between the outlet and inlet pressures of the fluid in the total compression train, n
 320 is the number of compression stages and ΔP_{HE} is the pressure drop (set to 0.1 bar) in every
 321 intercooler.

$$P_n = P_{n-1} \left(\frac{P_{out}}{P_{in}} \right)^{\frac{1}{n}} + \Delta P_{HE} \quad (6)$$

322 The outlet temperature from intercoolers has been fixed to 30°C.

323

324 3. Methods

325 The energy analysis and the comparison of the different proposed process solutions have been
326 performed by means of the net equivalent methane approach [23] that accounts for the amount of
327 biomethane required by defined reference processes to deliver thermal and mechanical energy to
328 each one of the analyzed processes. The aim is to reduce to the same basis the involved energy
329 contributions, ensuring a coherent assessment of the performances for each process.

330 Heat and mechanical works have been converted into the corresponding amounts of CH₄ required to
331 produce the same duty. In the examined processes, energy is supplied and/or removed at different
332 temperature levels. When low or cryogenic temperatures are required, the cooling duty has been
333 assumed to be produced by a proper refrigeration cycle, while when heat at temperatures around
334 100-150°C is needed, the thermal duty has been considered as low-pressure (LP) steam produced
335 by a CH₄-fired boiler. The heat removed from streams at temperatures higher than 100°C has been
336 assumed equal to the one of an equivalent LP steam potentially available for further uses into the
337 process. The mechanical work produced by turbines or required by compressors and pumps has
338 been considered as electric energy obtained by means of an equivalent CH₄-fired combined cycle
339 power plant.

340 The net energy consumption of each process has been determined, in this way, as the net CH₄
341 requirement. Energy consumptions (refrigeration, heating at high temperatures, compression and
342 pumping) have been assumed as CH₄ consumptions, while energy productions (turbine expansions
343 or heat removed at high temperatures) have been accounted as CH₄ productions.

344 When an energy stream is used to heat a process stream over the ambient temperature, it has been
345 related to the thermal energy generated by a boiler fed with CH₄ and producing LP steam, according
346 to eq. (7), where \dot{Q} is the thermal power, η_B is the boiler efficiency, LHV_{CH_4} is the lower heating
347 value of methane and \dot{m}_{CH_4} is the equivalent flowrate of biomethane required by the boiler.

$$\dot{m}_{CH_4} = \frac{\dot{Q}}{\eta_B \cdot LHV_{CH_4}} \quad (7)$$

348 When cooling at low temperatures is needed, a real refrigeration cycle has been considered. Its
349 Coefficient Of Performance (COP_f) has been calculated starting from the theoretical ideal one
350 ($COP_{f,id}$), obtained from the Carnot ideal cycle definition [29], corrected by a second law efficiency
351 defined as the ratio between the actual thermal efficiency and the maximum possible (reversible)
352 one at the same conditions [30]. It is a measure of how the performances of an actual process
353 approximate the ones of the corresponding reversible process [31]. In this way, the request of
354 cooling duty is calculated in terms of the equivalent CH₄ necessary to supply mechanical power to

355 the refrigeration cycle compressors. This energy has been assumed as electric energy produced by a
 356 CH₄-fired combined cycle power plant. The theoretical ideal *COP* can be calculated according to
 357 eq. (8), where T_0 is the ambient temperature (25°C) and T is the required low-temperature level.

$$COP_{f,id} = \frac{1}{\frac{T_0}{T} - 1} \quad (8)$$

358 The *COP* of the real refrigeration cycle is given by eq. (9), where η_{II} denotes the second law
 359 efficiency. The COP_f also represents the ratio between the provided cooling duty (\dot{Q}_{Cold}) and the
 360 electrical energy consumed (\dot{W}_{EL}) by the cycle (eq. (10)).

$$COP_f = COP_{f,id} \cdot \eta_{II} \quad (9)$$

$$COP_f = \frac{\dot{Q}_{Cold}}{\dot{W}_{EL}} \quad (10)$$

361 To transform the cooling duty into the equivalent CH₄ consumption, it is necessary to calculate the
 362 mechanical work required by the refrigeration cycle. CH₄ is then calculated according to eq. (11),
 363 where η_{CC} is the efficiency of the combined cycle, defined as the ratio between the net power output
 364 and the thermal power input coming from CH₄ combustion.

$$\dot{m}_{CH_4} = \frac{\dot{W}_{EL}}{\eta_{CC} \cdot LHV_{CH_4}} = \frac{\dot{Q}_{Cold}}{COP_f \cdot \eta_{CC} \cdot LHV_{CH_4}} \quad (11)$$

365 The powers related to pumps, turbines and compressors have been calculated (eq. (12)) in terms of
 366 equivalent CH₄ considering the same assumption adopted for the mechanical power in the
 367 refrigeration cycle.

$$\dot{m}_{CH_4} = \frac{\dot{W}_{EL}}{\eta_{CC} \cdot LHV_{CH_4}} \quad (12)$$

368 The values adopted for the lower heating value of methane, the efficiencies of combined cycle and
 369 boiler, the second law efficiency for refrigeration cycles and the *COP* of real refrigeration cycles,
 370 are listed in Table 1.

371

372 **Table 1.** Values of the parameters used to calculate the biomethane equivalent to process energy
 373 streams.

Parameter	Parameter Value	Reference
LHV_{CH_4} [MJ/kg]	50	[32]
η_{CC} [-]	0.55	[33]
η_B [-]	0.8	[34]
η_{II} [-]	0.6	[35]
COP_f (@ -165°C) [-]	0.34	This Work
COP_f (@ -100°C) [-]	0.83	This Work
COP_f (@ -35°C) [-]	2.38	This Work
COP_f (@ -10°C) [-]	4.51	This Work

374

375 **4. Results and discussion**

376 The method previously outlined has been applied to the studied process configurations for
 377 comparing their relative performances in terms of net equivalent biomethane. In order to extend and
 378 generalize the results, the net equivalent biomethane can be expressed in terms of percentage of
 379 produced biomethane useful to supply energy to the process (eq. (13)).

$$\%_{LBM} = \frac{\dot{m}_{CH_4}^{Produced} - \dot{m}_{CH_4}^{Consumed}}{\dot{m}_{CH_4}^{Produced}} \quad (13)$$

380 The results of the overall performances of the different processes are reported in Table 2.

381

382 **Table 2.** Percentages of the total produced biomethane required by the different investigated
 383 processes for LBG production.

Process	$\%_{LBM}$
Ryan-Holmes	15.70
Dual pressure low-temperature distillation	14.00
Anti-sublimation	21.79
MEA scrubbing	29.00

384

385 Low-temperature processes require to use a lower amount of the produced biomethane to supply
 386 energy to the process. Among them, the anti-sublimation process is the most energy-intensive, since
 387 the operation is performed by means of a direct phase change (frosting) in a single unit operation,
 388 where the cold utility is at constant temperature. On the contrary, operations based on distillation

389 (like the Ryan-Holmes and the dual pressure low-temperature distillation processes) are
 390 characterized by a space-distributed energy profile allowing a better use of cold utilities. The
 391 process with the lowest energy consumptions is the dual pressure low-temperature distillation
 392 process, while the Ryan-Holmes process is slightly more energy-intensive. This is due to the heat
 393 required for solvent regeneration that occurs at high temperature (137°C, as shown in Fig. 1).
 394 The contributions to the energy performances of each process can be better analysed in two ways:
 395 energy distribution by quality (mechanical power, cooling and heat duties) and energy distribution
 396 by operation (biogas compression, upgrading, CO₂ pressurization and biomethane liquefaction).
 397 As for the energy distribution by quality, the results in terms of percentages of the total energy
 398 requirements are reported in Table 3 for each of the investigated processes.

399
 400 **Table 3.** Distribution of the energy consumptions by quality.

Process	Mechanical power consumption [%]	Cooling consumption [%]	Heating consumption [%]
Ryan-Holmes	33.55	54.37	12.07
Dual pressure low- temperature distillation	38.77	61.23	0.00
Anti-sublimation	0.16	99.84	0.00
MEA scrubbing	7.78	34.82	57.40

401
 402 If the dual pressure low-temperature distillation process is compared with the Ryan-Holmes
 403 process, the former requires the highest mechanical power as a result of the higher pressure the raw
 404 biogas is compressed to (50 vs. 40 bar). Moreover, the dual pressure low-temperature distillation
 405 process also requires the highest cooling duty since it employs two condensers operated at low
 406 temperatures for performing the desired purification, while in the Ryan-Holmes process only one
 407 condenser at low temperature is needed. The disadvantage of the Ryan-Holmes process is the need
 408 of heat (LP steam) for solvent regeneration at about 137°C, which accounts for 12% of the total
 409 energy demand. On the contrary, for the reboiler of the HP section of the dual pressure low-
 410 temperature distillation process water can be used as service fluid to provide heat, since the
 411 temperature level is 15°C. For these two low-temperature processes, the mechanical power that can
 412 be recovered inside the process by means of the expander does not play a significant role: it is about
 413 3% of the total energy consumptions and about 8% of the mechanical power consumptions.
 414 For the anti-sublimation process all the energy requirements are concentrated in the cooling duty

415 demand, whereas for the MEA scrubbing process more than half of the total energy consumption is
 416 related to the heat required for solvent regeneration.

417 In Table 4, the distribution of the energy consumptions per type of operation is shown for each
 418 studied process solution. The distribution is expressed in terms of percentages of the total energy
 419 demand.

420
 421 **Table 4.** Distribution of the energy consumptions per type of operation.

Process	Biogas compression [%]	Biogas upgrading [%]	CO₂ pressurization [%]	Biomethane liquefaction [%]
Ryan-Holmes	33.41	39.74	0.12	26.74
Dual pressure low-temperature distillation	38.19	31.93	0.00	29.88
Anti-sublimation	0.00	73.99	0.16	25.85
MEA scrubbing	0.00	57.40	7.78	34.82

422
 423 Considering this second analysis, it is possible to notice that for low-temperature processes the
 424 contribution of the CO₂ pressurization is mostly negligible, since it is carried out by means of
 425 pumps due to the availability of carbon dioxide in liquid phase. The contribution of biomethane
 426 liquefaction to the total energy requirements is similar for each considered process configuration: it
 427 lies between 25 and 30%. For biogas compression the results are analogous to the ones reported in
 428 Table 3 for the mechanical power consumptions. The biggest difference among the three low-
 429 temperature processes is given by the biogas upgrading step: anti-sublimation has the highest power
 430 consumption since CO₂ is frosted in a single unit operation that uses entirely a single cold utility at
 431 constant temperature, while the two distillation processes need half of the energy requirements of
 432 the anti-sublimation. Considering only the two distillation-based processes, the energy required by
 433 the dual pressure low-temperature process is 10% less than that involved in the Ryan-Holmes
 434 process since no heat duties at high temperatures are required.

435 If the amine scrubbing process is taken into account, the results summarized in Table 4 suggest that
 436 the energy required for upgrading the raw biogas stream is higher in comparison with that related to
 437 the two less energy-demanding low-temperature processes (*i.e.*, the dual pressure low-temperature
 438 distillation process and the Ryan-Holmes process) due to the duty to be supplied to the reboiler of
 439 the *Regenerative distillation* column for solvent regeneration. The biomethane liquefaction step has

440 a share of the total energy consumption which does not significantly differ from the ones of the
441 same type of operation performed in low-temperature processes. On the contrary, the CO₂
442 pressurization step accounts to the total energy consumption to a larger extent than in low-
443 temperature processes due to the inter-refrigerated multistage compression train that is necessary to
444 bring the atmospheric CO₂ gaseous stream coming from the top of the *Regenerative distillation* unit
445 to the desired pressure of 50 bar.

446 Considering the results obtained in this study in terms of energy performances, there is a good
447 margin between the low-temperature processes and the MEA scrubbing process, especially for the
448 Ryan-Holmes and the dual pressure low-temperature distillation processes (*i.e.*, for the upgrading
449 processes based on low-temperature distillation), which exploit the synergy between the
450 temperature levels at which the upgrading and the liquefaction processes are operated.

451

452 **5. Conclusions**

453 In this work, the production of liquid biomethane (LBM) by the upgrading and liquefaction of
454 biogas has been studied considering three low-temperature purification technologies (*i.e.*, the Ryan-
455 Holmes extractive distillation process, a recently developed dual pressure low-temperature
456 distillation process and the anti-sublimation process) and the conventional amine scrubbing process,
457 by means of a MEA aqueous solution. These processes have been compared in terms of energy
458 consumptions evaluated by means of the net equivalent methane approach, which consists in
459 determining the amount of biomethane that is consumed within each process to supply the required
460 thermal and mechanical duties. The results of the comparison have been presented in terms of the
461 percentage of the produced biomethane required by each process for LBM production. Moreover,
462 the comparison has been also made by considering the contributions to the global energy
463 requirements distinguished by type of energy (*i.e.*, mechanical, cooling and heating) and by type of
464 operation (*i.e.*, biogas compression, biogas upgrading, CO₂ pressurization and biomethane
465 liquefaction). The performed analysis suggests that low-temperature processes, and the dual
466 pressure low-temperature distillation process in particular, have better performances than the
467 conventional amine scrubbing process, being the low temperatures reached in the upgrading step
468 synergistic to the production of liquid biomethane.

469

470 **References**

- 471 [1] R.E. Dugas, Pilot plant study of carbon dioxide capture by aqueous monoethanolamine, MSE
472 Thesis, University of Texas at Austin (2006).
473 [2] G. Xu, A.M. Scurto, M. Castier, J.F. Brennecke, M.A. Stadtherr, Reliable computation of high-
474 pressure solid-fluid equilibrium, *Industrial & engineering chemistry research* 39(6) (2000) 1624-

475 1636.
476 [3] M. Seiler, J. Groß, B. Bungert, G. Sadowski, W. Arlt, Modeling of solid/fluid phase equilibria in
477 multicomponent systems at high pressure, *Chemical engineering & technology* 24(6) (2001) 607-
478 612.
479 [4] M. Persson, O. Jönsson, A. Wellinger, Biogas upgrading to vehicle fuel standards and grid
480 injection, IEA Bioenergy task, 2006.
481 [5] T. Eggeman, S. Chafin, Pitfalls of CO₂ freezing prediction, Proceedings of the 82nd Annual
482 Convention of the Gas Processors Association, San Antonio, TX, USA, 2003.
483 [6] B. ZareNezhad, T. Eggeman, Application of Peng–Rabinson equation of state for CO₂ freezing
484 prediction of hydrocarbon mixtures at cryogenic conditions of gas plants, *Cryogenics* 46(12) (2006)
485 840-845.
486 [7] V. Feroiu, O. Partenie, D. Geana, Modelling the solubility of solid aromatic compounds in
487 supercritical fluids, *Rev. Chim.* 61 (2010) 685-690.
488 [8] X. Tang, J. Gross, Modeling the phase equilibria of hydrogen sulfide and carbon dioxide in
489 mixture with hydrocarbons and water using the PCP-SAFT equation of state, *Fluid Phase Equilibria*
490 293(1) (2010) 11-21.
491 [9] S. Taotao, L. Wensheng, Calculation of carbon dioxide solubility in liquefied natural gas,
492 *International Journal of Chemical Engineering and Applications* 2(5) (2011) 366.
493 [10] S. Gamba, L. Pellegrini, Biogas upgrading: Analysis and comparison between water and
494 chemical scrubbing, *Chemical Engineering Transactions*, 32 (2013) 1273-1278.
495 [11] G. Bortoluzzi, M. Gatti, A. Sogni, S. Consonni, Biomethane Production from Agricultural
496 Resources in the Italian Scenario: Techno-Economic Analysis of Water Wash, *Chemical*
497 *Engineering Transactions*, 37 (2014) 259-264.
498 [12] Y. Koga, L. Harrison, *Comprehensive chemical kinetics*, Bamford, CH, Tipper, CFH,
499 Compton, RG (Eds.) 21 (1984) 120.
500 [13] B. Kelley, J. Valencia, P. Northrop, C. Mart, Controlled Freeze Zone™ for developing sour gas
501 reserves, *Energy Procedia* 4 (2011) 824-829.
502 [14] A.S. Holmes, J.M. Ryan, Cryogenic distillative separation of acid gases from methane, Google
503 Patents, 1982.
504 [15] A.S. Holmes, J.M. Ryan, Distillative separation of carbon dioxide from light hydrocarbons,
505 Google Patents, 1982.
506 [16] L.A. Pellegrini, Process for the removal of CO₂ from acid gas, Google Patents, 2014.
507 [17] I. Kikic, M. Lora, A. Bertucco, A thermodynamic analysis of three-phase equilibria in binary
508 and ternary systems for applications in rapid expansion of a supercritical solution (RESS), particles
509 from gas-saturated solutions (PGSS), and supercritical antisolvent (SAS), *Industrial & engineering*
510 *chemistry research* 36(12) (1997) 5507-5515.
511 [18] J. Richardson, B. Turk, M. Twigg, Reduction of model steam reforming catalysts: effect of
512 oxide additives, *Applied Catalysis A: General* 148(1) (1996) 97-112.
513 [19] AspenTech, Aspen Hysys®, AspenTech, Burlington, MA, 2012.
514 [20] G. Soave, Equilibrium constants from a modified Redlich-Kwong equation of state, *Chemical*
515 *Engineering Science* 27(6) (1972) 1197-1203.
516 [21] V. Vinš, A. Jäger, J. Hrubý, R. Span, Phase equilibria of carbon dioxide and methane gas-
517 hydrates predicted with the modified analytical SLV equation of state, *EPJ Web of Conferences*,
518 EDP Sciences, 2012, p. 01098.
519 [22] J.B. Klauda, S.I. Sandler, Ab initio intermolecular potentials for gas hydrates and their
520 predictions, *The Journal of Physical Chemistry B* 106(22) (2002) 5722-5732.
521 [23] A. Martin, C. Peters, New thermodynamic model of equilibrium states of gas hydrates
522 considering lattice distortion, *The Journal of Physical Chemistry C* 113(1) (2009) 422-430.
523 [24] M.A. Mahabadian, A. Chapoy, R. Burgass, B. Tohidi, Development of a multiphase flash in
524 presence of hydrates: Experimental measurements and validation with the CPA equation of state,

525 Fluid Phase Equilibria 414 (2016) 117-132.
526 [25] A.L. Kohl, R. Nielsen, Gas purification, Gulf Professional Publishing 1997.
527 [26] S. Langè, L.A. Pellegrini, P. Vergani, M. Lo Savio, Energy and Economic Analysis of a New
528 Low-Temperature Distillation Process for the Upgrading of High-CO₂ Content Natural Gas
529 Streams, Industrial and Engineering Chemistry Research 54(40) (2015) 9770-9782.
530 [27] M. Yazdizadeh, A. Eslamimanesh, F. Esmaeilzadeh, Thermodynamic modeling of solubilities
531 of various solid compounds in supercritical carbon dioxide: Effects of equations of state and mixing
532 rules, The Journal of Supercritical Fluids 55(3) (2011) 861-875.
533 [28] J. Lennard-Jones, A. Devonshire, Critical phenomena in gases. II. Vapour pressures and boiling
534 points, Proceedings of the Royal Society of London. Series A, Mathematical and Physical Sciences
535 (1938) 1-11.
536 [29] J. Lennard-Jones, A. Devonshire, Critical phenomena in gases. I, Proceedings of the Royal
537 Society of London. Series A, Mathematical and Physical Sciences (1937) 53-70.
538 [30] A. Lyngfelt, B. Leckner, T. Mattisson, A fluidized-bed combustion process with inherent CO₂
539 separation; application of chemical-looping combustion, Chemical Engineering Science 56(10)
540 (2001) 3101-3113.
541 [31] M.M. Hossain, H.I. de Lasa, Chemical-looping combustion (CLC) for inherent CO₂
542 separations—a review, Chemical Engineering Science 63(18) (2008) 4433-4451.
543 [32] R.H. Perry, D.W. Green, Perry's chemical engineers' handbook, 7th ed., New York: McGraw-
544 Hill. 2008.
545 [33] A. Chakma, CO₂ capture processes - Opportunities for improved energy efficiencies, Energy
546 Conversion and Management 38 (1997) S51-S56.
547 [34] L.A. Pellegrini, S. Moioli, S. Gamba, Energy saving in a CO₂ capture plant by MEA scrubbing,
548 Chemical Engineering Research and Design 89(9) (2011) 1676-1683.
549 [35] S. Moioli, L. Pellegrini, S. Gamba, Simulation of CO₂ capture by MEA scrubbing with a rate-
550 based model, Procedia Engineering 42 (2012) 1651-1661.
551
552
553